



Multiphysics finite element analysis of limestone dissolution

Case study: Northern plains limestone bed of Hamedan

#	Name	Email Address	Degree	Position	Country	Affiliation
1	Hossein Pour Hamedani, Hossein	cenano_2010@yahoo.com	Ph.D. Candidate	Other	Iran	Civil Engineering Department, Bu-Ali Sina University Hamedan, Iran
2	Maleki, Mohammad	maleki@basu.ac.ir	Ph.D.	Associate Professor	Iran	Civil Engineering Department Bu-Ali Sina University Hamedan Iran

Received: 06/09/2023

Revised: 26/04/2024

Accepted: 21/07/2024

Abstract

Fluid transformation in the karst bed leads to enlarged voids and cavities and increases the risk of instability and consequently, catastrophic events such as sinkholes may occur. In this paper, the dissolution of limestone was simulated numerically by using a finite element code capable of taking into account multi-physics governing equations and mesh moving and updating. In the first step, the finite element code was identified based on dissolution experimental results concerning three regions of Hamekasi, Ali Sadr and Abshineh in the northern plains of Hamedan city. In the second step, geometrical changes of a vertical cavity in the dissolution process during time for the mentioned limestone beds were studied and compared. The results showed that the proposed numerical modeling has very good capabilities in reproducing experimental data. The results of the dissolution in a vertical hole indicate that entering fluid velocity in comparison with the initial diameter cavity, plays an important role in the hole widening. The widening trend of the hole in the inlet and outlet sections is the same for different initial hole diameters, however, the width of the inlet section of the flow is greater than the width of the middle and outlet sections.

Keywords: Limestone; Dissolution; Numerical simulation; COMSOL Multiphysics

1. Introduction

Karst formations are the product of the dissolution of soluble rocks and are of special importance. The main consequences of bedrock dissolution include sinkholes, the creation of valleys and dry pits, cave systems and underground holes, especially in the spring season, and can disrupt the ground conditions for construction engineering and even agriculture and other human activities (Waltham, et al. 2005). Soluble bedrock includes several formations such as chalk, salt, and, limestone, however, limestone is called the most primitive formation of sinkholes (Taheri et al., 2015).

The dissolution of soluble rocks has been mainly investigated experimentally (e.g. Zhang et al., 2022, Min et al., 2022, Novack et al., 2022, Meng et al., 2023). The literature review shows that dissolution intensity is directly proportional to dissolution time, flow rate, temperature, and hydrodynamic pressure, H^+ concentration, and inversely proportional to pH value. However, concerning the analytical or numerically mathematical predictions of the dissolution behavior of soluble rocks there

are very few studies in comparison with experimental works (e.g. Farrokhrouz et al., 2022, Balazi et.al 2022, Ferreira et al., 2020, Zhao, et al. 2018, Shovkun and Espinoza, 2019, Schabernack and Fischer, 2022, Xiao-Lei et al., 2023, Zhang et al., 2022, Luo et al., 2014; Laouafa, et al. 2021, Zhang et al., 2019, Agrawal et al., 2020, Orgogozo et al., 2010; Laouafa et al., 2012; Ogata et al., 2018; Wang et al., 2020). Farrokhrouz et al., (2022) presented an analytical solution for the reactive diffusion of mineral dissolution when acid is absorbed to the rock surface and investigated porosity changes. The mathematical modeling contains a diffusion-based continuity equation without an advection term. They carried out certain experiments on Indiana limestone for validation of their analytical solution. Balazi et al. (2022) presented an explicit finite element method for solving the Navier-Stokes Brinkman equations and studied the effect of the microporosity field using the Kozeny-Carman relation and showed that small change in microporosity has a significant effect on the effective permeability. Ferreira et al., (2020) have studied the contribution of each term in the Navier-Stokes-Darcy equation (Brinkman equation) in the fluid linear momentum balance and investigated the consequences of choosing the Darcy or Brinkman equations in three-dimensional simulations of the reactive flow of a strong carbonate. They found that the convective acceleration term in the Brinkman equation plays an important role in describing the fluid momentum balance at high induced velocities. Shovkun and Espinoza, (2019) have solved the equations for fluid flow, pore elasticity, linear elastic fracture mechanics, and reactive transport through numerical simulation using finite element method.

In recent years advanced computational codes have been used for the modeling of physico-chemical effects during the dissolution process (Schabernack and Fischer, 2022, Xiao-Lei et al., 2023, Zhang et al., 2022, Luo et al., 2014; Laouafa, et al. 2021, Zhang et al., 2019, Agrawal et al., 2020, Laouafa, et al. 2021). Based on the literature reviews, in the majority of the works, the finite element COMSOL Multiphysics code was used as a strong tool for solving governing equations. This code is capable of modeling diverse physical and chemical aspects in a given domain with

complex boundary conditions. As an example, Zhang et al., (2022) coupled the Darcy-Brinkman-Stokes with the geochemical modulus and stated that advection can lead to spatial changes in the local dissolution rate of dolomite, however, it was not significantly influenced by the chemistry of the material.

A few numbers of studies were also effectuated for predicting the expansion of the hole in bedrock due to dissolution on a macro-scale (Orgogozo et al., 2010; Laouafa et al., 2012; Ogata et al., 2018; Wang et al., 2020). This route is important because hole development leads to collapse in bedrock and overburden soil.

Oligocene–Miocene Qom Formation in central Iran is a regional transgressive-regressive sequence that is bounded by two continental units Lower and Upper Red formations. This formation especially in the north and northwest of Hamedan, is highly susceptible to the creation of sinkholes (Karimi and Taheri, 2010; Taheri et al., 2015; Delkhahi et al., 2020). Hamadan is a city located in the west of Iran (Fig.1), and in the last two decades, the occurrence of sinkholes in its north and northwest plains has spread and caused many dangers. The karst and limestone bed of these plains, the drop-down in the underground water level, and its dissolution are some of the most important factors in the creation of holes and their development. The drop of the underground water level in these areas in 25 years leading to the 2000s decade has been more than 70 meters. The first identified sinkhole was in the village of Hamekasi, in the city of Qahavand, with a depth of 2 meters and a diameter of 34 meters in the year 1992. During the following twelve years, 36 sinkholes with various depths between 8 and 21 meters and diameters of 14 to 30 meters have occurred in the northwestern area of this plain (Taheri et al. 2005). The most common type of sinkholes occurring in the northern plains of Hamedan is dissolution and rupture. Areas with karst lithology are mainly composed of three types of salt bedrock, chalk or limestone. The study of the lithology of the bedrock of these areas reveals the existence of five morphological categories related to karstification potential, including limestone, marly limestone, marls, conglomerate, sandstone, and schist-shale (Taheri et al.

2005). According to Taheri et al., 2015, areas with limestone beds have the highest potential and areas with schist-shale beds have the lowest karst potential. Based on the experiments (Delkhahi et al., 2020), the dominant geological structure of these regions is the limestone of the Qom Formation (Oligo-Miocene), and carbonate dissolution is dominant in this region.

In this paper, the dissolution processes of limestone, situated in the north and northwest of Hamedan, were investigated. The governing equations were solved using the Multiphysics finite element code of COMSOL 6.0. In the first step finite element code was calibrated based on existing experimental data for three regions of Hamekasi, Ali-Sadr, and Abshineh. Then, the rate of dissolution for a vertical cylindrical hole with different diameters was predicted and compared for the three mentioned regions. Based on the literature review this study is the first try regarding numerical modeling of limestone dissolution related to the northern plains of Hamedan and covers its innovation.

2. Governing equations and mathematical model

The governing equations consist of mass and linear momentum conservations of the fluid and the mass transfer equations of the reacting components. In this study, it is assumed that the phases are continuous and fluid is Newtonian, isothermal and temperature is constant.

2.1. Equations governing fluid flow

Conservation of momentum and mass of components in the fluid phase is expressed by Navier-Stokes equations for fluid flow and advection-diffusion equations for solute transport. The general state of the Navier-Stokes equations for incompressible flow is as follows (Sheng, 2013);

$$\rho \frac{D\mathbf{u}}{Dt} = \rho \mathbf{g} - \nabla P + \mu \nabla^2 \mathbf{u} \quad (1)$$

$$\nabla \cdot \mathbf{u} = 0 \quad \rightarrow \quad \frac{\partial \mathbf{u}}{\partial t} + \nabla \cdot (\mathbf{u}\mathbf{u}) = -\frac{1}{\rho} \nabla p + \vartheta \nabla^2 \mathbf{u} \quad (2)$$

In these equations, \mathbf{u} is the fluid velocity vector and p is the fluid pressure. ρ is the density and ϑ is the kinematic viscosity of the fluid and it is assumed that both are independent of the

concentration of the solution. The transfer of dissolved substances by the fluid in the fluid phase is expressed by the following equation called the diffusion-advection equation (Molins et al., 2021).

$$\frac{\partial C}{\partial t} + \nabla \cdot (\mathbf{u}C) = D_m \nabla^2 C \quad (3)$$

where C is the solute concentration and D_m is the molecular diffusion coefficient. The temperature is assumed to be constant.

2.2. Mass transfer at the fluid-solid interface

In this research, it is assumed that chemical reactions are carried out only at the fluid-solid interface. For the first time Plummer, et al., (1978) expressed the reaction mechanism on the surface of calcite with the presence of carbonic acid in a simplified form as the following equation.



In addition to the dissolution equilibrium chemistry, which is well described in previous studies (e.g. Dreybrodt 1988, 2000, Morse & Mackenzie, 1990) dissolution rate is also very important in the limestone dissolution system. Various parameters that control the rate of dissolution rate of rock are solubility, the dissolution rate constant of constituent mineral components, the degree of saturation of the solvent liquid, the amount of space for solvent liquid, and its motion (Arvidson *et al.*, (2003)). Several empirical relationships already exist in the literature for estimating the dissolution rate of limestone due to water transformation (Plummer et al (1978), Palmer (1991, 2016), Kaufmann and Dreybrodt, 2007, Kaufmann, et al. 2019).

Based on the literature review and comparison of various propositions, in the present study, the following relationship was considered to calculate the kinetics of dissolution limestone.

$$R_{diss} = k_s(1 - c_{ca}/c_{eq})^n \quad (5)$$

Where, R_{diss} is the dissolution reaction rate in moles per square meter per second, which indicates the rate of separation of materials from the contact surface of water with limestone per

second. k_s is the computational dissolution rate constant in terms of moles per square meter per second. c_{ca} and c_{eq} are the concentration of calcium ions in the solution in the current and equilibrium state respectively. Both of c_{ca} and c_{eq} are in terms of milligrams per liter. The parameter n controls the nonlinear trend of the dissolution intensity. As seen from equation (5), when c_{ca} reaches c_{eq} , $R_{diss}=0$, and the dissolution process is stopped. In this research, the deposition of particles during and after the dissolution process was not taken into account.

3. Analysis method

In dissolution processes, the transfer of reactants is done by diffusion and advection relative to the dissolution surface and subsequently, the ions are separated from the solid surface and pass through the diffusion and advection boundary layer by fluid movement (Dreybrodt et al., 1996; Golfier et al., 2002; Colombani, 2008, Guo 2015). The dissolution process is controlled by the slowest mechanism. If the mass transfer from or to the dissolution surface is slower than the dissolution rate, the dissolution process is mass transfer-limited, and transfer is the controlling mechanism, while if the reaction kinetics is very slow, the dissolution process is reaction-limited, and reaction is the controlling mechanism. Accordingly, the dissolution of rock salt due to the high velocity of its reaction kinetics is mass transfer-limited and the dissolution process of carbonate and sulfate rocks (such as gypsum) is controlled by comparing the velocity of a chemical reaction and mass transfer (Golfier et al., 2002; Colombani, 2008; Laouafa et al., 2015). Therefore, limestone dissolution processes are a chemical and physical phenomenon and its numerical analysis should be done as a problem with multiple physics. Due to the change in the geometry of the Rock surface due to dissolution, the finite element code must be able to consider mesh moving and mesh upgrading.

Many scientific and engineering problems require the use of numerical methods and algorithms to obtain computational simulation results because analytical solutions are rarely available for them. The problem of instability of chemical dissolution in fluid-saturated porous rocks is not an exception to this rule (Zhao, et al. 2018). Computational fluid dynamics (CFD) softwares,

such as COMSOL Multiphysics, is one of the tools for numerical analysis of problems related to fluid flow in porous media with chemical reactions, such as limestone dissolution. This software works based on the finite element method and can analyze various physics and engineering applications, especially coupled phenomena. In this article, to simulate the dissolution of limestone and the transfer of the resulting materials, which is considered a reactive transfer process, three different physics of COMSOL software were used knowing that fluid concentration and velocity were selected as basic variables. The physics of transfer of dilute components (TDS), is considered to simulate the reaction process. The physics of Darcy flow or creep flow (DF, CF) was selected to investigate and simulate the fluid flow in the carbonate rock mass and finally, to change the geometry during the analysis in the dissolved part and the fluid domain, moving mesh (MM) physics, was used. All three physics in the static and time-dependent analysis are coupled and their interactions are taken into account.

4. Calibration of the multiphysics finite element code

The results of laboratory tests related to the dissolution of limestones of Hamekasi, Abshineh, and Ali Sadr carried out by Doosti (2018) were used to calibrate multiphysics finite element code. These three areas are located in the northern plains of Hamedan and situated on limestone bedrock. Besides civil and agricultural activities, many important industrial factories, infrastructure, and facilities such as Shahid Mofateh Power Plant, Abshineh Dam, and Ali-Sadr Cave the largest water cave in the world situated in these regions. So far, a significant number of sinkholes have occurred in the northern plains of Hamedan which reveals the necessity and importance of research in this field. The number of samples collected from the Hamekasi, Ali Sadr, and Abshineh areas are 39, 34, and, 40 respectively. The tests were carried out using an improved circulation device and the acidity of the water inside the tank was constant during the test. The tests were performed under three levels of pH equal to 6.7, 7.2, and, 7.7 for each of the three regions. The water temperature in the tank was also kept constant according to local conditions about 2 to 5 Celsius degrees. In the

laboratory, the dissolution rate constant for each region has been measured using the circulation method. To calculate the laboratory dissolution rate constant, James and Lupton (1978) method has been used according to the following equation.

$$\frac{dm}{dt} = K_c A (c_{eq} - c) \quad (6)$$

In which, dm/dt is the time rate of mass change, K_c is the laboratory dissolution rate constant, A is the surface of the rock in the vicinity of water, c_{eq} is the calcium ion concentration in the saturated state (equilibrium) and c is the calcium ion concentration at any time.

The laboratory results of determining the dissolution rate constant for the three regions are collected in Table 1. The graphs of calcium ion concentration changes measured during the experiments are shown in Fig. 2.

4.1. Tests modeling in COMSOL

The parameters related to the dissolution relationship (Eq. 5), were determined for the three studied areas by simulating the tests conditions. Figure 3 (a) shows the arrangement of the samples simulated in COMSOL. The selected elements for the three-dimensional analysis of the dissolution of rock samples are Tetrahedral so that near the interface with fluid, a much finer mesh has been selected to avoid possible errors and achieve the convergence of the results. For the numerical analysis of the two-dimensional fluid flow, the Triangular elements have been used so that the size of elements is larger in the solid far from the fluid and finer meshing is used for the boundaries where the exchange of particles from the rock into the fluid takes place. Based on COMSOL recommendation before main time-dependent analyses, a stationary analysis has been done approving selected meshing. To save time analyses, the symmetrical geometry was considered in both horizontal and vertical directions, which is shown in Fig. 3 (b, c, d).

The concentration of calcium ions in the inlet flow taken from the laboratory diagrams (Fig. 2), was applied as the initial concentration parameter at any moment at the inlet section as one of the boundary conditions ($C_i = C_0$). The initial velocity of the fluid was also applied to the inlet boundary.

In the interface between the samples and the fluid as a reactive surface, the kinetic boundary conditions of the dissolution reaction were applied according to equation (5). On the lateral borders of the tank, the conditions of no flux and fluid flow and $\mathbf{u}=\mathbf{0}$ were applied. In the outlet section of the flow $\mathbf{n} \cdot D_m \nabla C=0$ and zero pressure were applied as boundary conditions. According to the symmetry considered for the model, the boundary conditions $-\mathbf{n} \cdot (\mathbf{J}_i + \mathbf{u}C) = 0$ and velocity balance ($\mathbf{u} \cdot \mathbf{n} = 0$) was applied in the symmetric boundaries. To consider the geometry change conditions during the dissolution of the rock surface, the boundary conditions of the dissolution parts in the samples change at a velocity equal to the dissolution rate, and other boundaries were considered fixed.

The parameters of the macroscopic transport equation are determined as a function of dimensionless numbers such as the Peclet number. The dimensionless Peclet number (Pe) compares the characteristic times of diffusion and convection and is defined as relation (7) where \mathbf{u} is the velocity of the fluid and l is the length of the flow path.

$$Pe = \frac{\mathbf{u} \cdot l}{D_m} \quad (7)$$

In equation (5) as dissolution kinetics, two parameters, dissolution rate constant (k_s) and reaction order (n) were determined through a set of simulations for each of the studied areas in such a way that the graphs obtained from numerical and laboratory studies relatively match. The calibration results for each of the studied areas are shown in Fig. 4. In these graphs, the mass changes of the total samples during the experiment were drawn and compared with the numerical analysis results. The values of pairs of parameters obtained from calibration are presented in Table 2.

5. Modeling the vertical hole widening in rock

Using the parameters obtained from the calibration of the finite element code presented in Table 2, the geometrical changes of a vertical hole in the bedrocks of Hamekasi, Ali Sadr, and Abshineh, were studied. The holes are subjected to the vertical movement of the fluid and the rate of dissolution will be captured numerically. The vertical holes were considered with three initial

diameters of 3, 6, and 12 mm. The meshed geometry of the model and fluid flow path are shown in Fig. 5. The problem was modeled for each of the areas with three different acidities (pH=6.7, 7.2, and 7.7) and under different values of the velocity of fluid flow entering the hole, which is increased tenfold in each analysis ($Pe=1e3, 1e4, 1e5$ and $1e6$).

Fig. 6 shows the results of the analyses carried out on the rock sample of the Hamekasi region at a pH equal to 6.7 and at the times of one day, one month, six months and one year from the beginning of dissolution, and Fig. 7 shows the evolution of the hole for the rock sample of the same region and with the same acidity but under the conditions of different flow velocities ($Pe=1e3, 1e4, 1e5, 1e6$). This trend has been obtained similarly for samples from other regions. The process of dissolution of the rock sample for each of the areas shows that the separation of solid particles and their transformation by fluid flow and the change of the geometry of the holes can be well simulated by COMSOL Multiphysics.

Looking more closely at the images in Fig. 7, we find that in low Peclet numbers (1000) after 16 days, the diffusion process is still dominant and due to the low velocity of the fluid flow, the dissolved substances have the opportunity to accumulate in the fluid environment. It seems that the reaction process dominates the transfer and this factor has caused the hole widening to be slower and with a smaller amount. With the increase in the velocity of the flow, the transition period gradually prevails and while the dissolved materials are transported faster from the surface of the limestone, their accumulation decreases, and with the decrease in the concentration of calcium ions in the solution due to its exit from the environment, a greater amount of the wall of the hole is dissolved. This indicates the holes that are subjected to a higher velocity will experience a greater change in the diameter of the hole at the inlet and outlet flow sections. On this basis, it can be expected that the maximum amount of widening or opening of the hole for the rock samples of the Hamekasi region will increase with the increase in the Peclet numbers which is evident in Fig. 8.

From the images in Fig. 8, it can be deduced that the process of widening in the inlet and outlet of the sample is the same for all cases of the initial diameter of the hole. In other words, the rate of dissolution is less affected by the initial diameter of the hole. However, in all cases, the width of the inlet section of the flow is greater than the width of the middle and outlet sections. Also, in low Peclet numbers, the ratio of the widening in the inlet section of the flow to its outlet section is significant, however, with the increase of the fluid velocity at the inlet, this ratio decreases and the group of graphs is closer to each other. In addition, the results show that increasing the velocity of the inlet fluid has a greater effect on the widening of the outlet section, and the slope of the curves for the outlet section is greater than that of the inlet.

Figure 9 shows the maximum mass reduction of samples after 16 days (23040 minutes) from the beginning of the dissolution process. In Fig. 9a, the mass reduction values due to the increase in Peclet number are plotted for the three regions with three different pHs and the initial diameter of the hole equal to 3 mm. The results show that similarly, for all cases, a 10-fold increase in the flow rate in four stages (from $Pe=1000$ to $Pe=1000000$) increases the dissolved mass of the samples by 2.3 to 5.7 times. Increasing the initial diameter of the hole by 2 times (initial diameters of 3, 6, and 12 mm) increases the lost mass of the stone by 1.5 to 3.5 times. From the graphs in Fig. 9, it can also be seen that at low values of Peclet number ($Pe=1000$), the effect of acidity on dissolution is insignificant, but with the increase of the fluid flow rate, the hole diameter in the samples that are exposed to a more acidic environment (lower pH) becomes more widened and opened. The acidic environment when the flow rate is higher can provide better conditions for more dissolution of the sample and more evolution of cavities. In general, according to the obtained results, the largest reduction in mass is related to the samples of the Abshineh region in the more acidic environment, and the least reduction in mass belongs to the Hamekasi region in high acidity conditions. This pattern corresponds similarly to the equilibrium saturation concentration of calcium ions in these regions. In other words, the samples from the Abshineh region that have a higher saturation concentration

experience a greater mass reduction with time. It seems that in the samples from the area of Hamekasi more time is required for dissolution and cavity evolution because the solution reaches the concentration equilibrium state sooner. Despite the calibration done, the difference in the mass reduction of the samples with the laboratory results can also be caused by the presence of impurities in the samples and their sedimentation pattern in the laboratory, which are not considered in the numerical study.

In Fig. 10, the ratio of the width changes of the inlet and outlet sections in terms of time for different entering fluid velocities for the Hamekasi samples is shown. At the beginning of dissolution and until the end of the first day, this ratio has an upward trend. In other words, at the beginning of the dissolution process, the opening of the inlet section is started however, the opening of the outlet flow is subjected to a certain delay until the fluid momentum is received. In the following, and passing time, a similar trend has been gradually created for the width changes of the input and output of the flow.

6. Conclusion

This paper aimed to investigate the mathematical modeling and numerical solution of the limestone dissolution process as one of the substrates prone to create sinkholes. For this purpose, after exploring the governing equations, using existing experimental results on rock samples from three regions of the Northern plains of Hamedan city the moduli and parameters of multiphysics finite element code were identified and calibrated. In the following dissolution process, cylindrical holes with different initial diameters subjected to various fluid velocities for the mentioned three regions were investigated. Considering that one of the important causes of sinkhole occurrence in the northern plains of Hamedan is related to the dissolution of limestone bedrock, therefore, the present work is an effective step in developing the studies in this field. The main results obtained from this paper are listed below:

1. A very good agreement was observed between the results of numerical simulations and those of laboratory tests. This confirms the capacity of the chosen framework to predict limestone bedrock solutions and their effects.
2. For the samples of each of the three regions, as the pH decreases, the calcium ion saturation concentration and the dissolution rate constant increase. This issue was well simulated by the proposed numerical framework.
3. By increasing the Peclet number, simultaneously with the mass reduction in all cases, the difference in mass reduction between different conditions increases significantly. Also, in all samples, the hole width increases with the increase of the flow velocity.
4. In general, compared to the initial diameter of the hole, a change in Peclet number and pH value has more influence on the widening of the hole due to the dissolution.
5. At low velocities of the inlet fluid flow, the effect of acidity is insignificant, however, increasing fluid velocity in lower pH leads to an increase in the dissolution effect and more widening of holes.
6. The widening trend of the hole in the inlet and outlet sections is the same for all cases of different initial hole diameters, however, in all cases, the width of the inlet section of the flow is greater than the width of the middle and outlet sections.
7. At low Peclet numbers, the ratio of widening in the inlet section of the flow to outlet section is significant, however, this ratio decreases with the increase of fluid velocity at the inlet.
8. The increase in fluid velocity has a greater effect on the width of the outlet section compared to the inlet section.
9. Increasing the initial diameter of the hole causes a small decrease in the ratio of width to initial diameter at the entrance section.

7. Acknowledgments

We would like to thank Mr. Manouchehr Doosti for providing the results of the experiments and also expressing his valuable opinions in line with the consistency of this study.

8. References

- Agrawal, P., Raof, A., Iliev, O. and Wolthers, M. (2020). "Evolution of pore-shape and its impact on pore conductivity during CO₂ injection in calcite: Single pore simulations and microfluidic experiments", *Advances in Water Resources*, 136. Doi: 10.1016/j.advwatres.2019.103480
- Arvidson, R. S., Ertan, I. E., Amonette, J. E. and Lutge, A. (2003). "Variation in calcite dissolution rates: A fundamental problem?", *Geochimica et Cosmochimica Acta*, 67: 1623–1634. doi:10.1016/S0016-7037(02)01177-8
- Balazi Atchy Nillama, L., Yang, J. and Yang, L. (2022). "An explicit stabilised finite element method for Navier-Stokes-Brinkman equations", *Journal of Computational Physics* (on-line), 457: 111033. Doi:10.1016/j.jcp.2022.111033
- Colombani, J. (2008). "Measurement of the pure dissolution rate constant of a mineral in water", *Geochimica et Cosmochimica Acta*, 72: 5634–5640. Doi:10.1016 /j.gca.2008.09.007
- Delkhahi, B., Nassery, H. R., Vilarrasa, V., Alijani, F. and Ayora, C. (2020). "Impacts of natural CO₂ leakage on groundwater chemistry of aquifers from the Hamadan Province, Iran", *International Journal of Greenhouse Gas Control*, 96. Doi: 10.1016/j.ijggc.2020.103001
- Dreybrodt, W.: (2000). "Equilibrium chemistry of karst waters in limestone terranes", *National Speleological Society, Huntsville*, 130-136.
- Dreybrodt, W., Lauckner, J., Zaihua, L., Svensson, U. and Buhmann, D. (1996). "The kinetics of the reaction CO₂ + H₂O → H⁺ + HCO₃⁻ as one of the rate limiting steps for the dissolution of calcite in the system H₂O-CO₂-CaCO₃", *Geochimica et Cosmochimica Acta*, 60: 3375–3381. Doi: 10.1016/0016-7037(96)00181-0
- Dreybrodt, W. (1988). "*Processes in karst systems: Physics, chemistry, and geology*", SpringerVerlag, Berlin.
- Doosti, M. (2009). "Geological engineering study of limestones in the north and northwest of Hamadan", Master's Thesis, University of BuAli Sina. (In Persian)
- Farrokhrouz, M., Taheri, A., Iglauer, S. and Keshavarz, A. (2022). "Laboratorial and analytical study for prediction of porosity changes in carbonaceous shale coupling reactive flow and dissolution", *Journal of Petroleum science and engineering*, 215. Doi: 10.1016/j.petrol.2022.110670
- Ferreira, L. de P., Oliveira, T. D. S. de, Surmas, R., da Silva, M. A. P. and Peçanha, R. P. (2020). "Brinkman equation in reactive flow: Contribution of each term in carbonate acidification simulations", *Advances in Water Resources*, 144. Doi:10.1016/j.advwatres.2020.103696
- Golfier, F., Zarcone, C., Bazin, B., Lenormand, R., Lasseux, D. and Quintard, M. (2002). "On the ability of a Darcy-scale model to capture wormhole formation during the dissolution of a porous medium", *Journal of Fluid Mechanics*, 457: 213–254. Doi: 10.1017/S0022112002007735
- Guo, J. (2015). "Numerical modeling of the dissolution of karstic cavities", PhD Thesis, University of Toulouse.
- James, A.N. and Lupton, A.R.R. (1978). "Gypsum and anhydrite in foundations of hydraulic structures", *Géotechnique*, 28(3), pp. 249–272. Doi: 10.1680/geot.1978.28.3.249
- Karimi, H. and Taheri, K. (2010). "Hazards and mechanism of sinkholes on Kabudar Ahang and Famenin plains of

- Hamadan, Iran", *Natural Hazards*, 55: 481–499. Doi: 10.1007/s11069-010-9541-6
- Kaufmann, G. and Dreybrodt, W. (2007). "Calcite dissolution kinetics in the system CaCO₃-H₂O-CO₂ at high undersaturation", *Geochimica et Cosmochimica Acta*, 71: 1398–1410. Doi:10.1016/j.gca.2006.10.024
- Kaufmann, G., Romanov, D. and Dreybrodt, W. (2019). Modeling the evolution of karst aquifers. *Encyclopedia of Caves*: 717–724. Doi: <https://doi.org/10.1016/B978-0-12-814124-3.00086-8>
- Laouafa, F., Guo, J. and Quintard, M. (2021). "Underground Rock Dissolution and Geomechanical Issues", *Rock Mechanics and Rock Engineering* (on-line), 54: 3423–3445. Doi: 10.1007/s00603-020-02320-y
- Laouafa, F., Guo, J., Quintard, M. and Luo, H. (2015). "Numerical modelling of salt leaching-dissolution process", In: *49th US Rock Mechanics / Geomechanics Symposium 2015*. Institut National de l'Environnement Industriel et des Risques-ENERIS, Verneuil-en-Halate, F-60550, France. pp.2126–2135.
- Laouafa, F., Luo, H., Quintard, M. and Debenest, G. (2012). "A numerical method for cavity dissolution in salt formation", In: *Mechanical Behavior of Salt VII - Proceedings of the 7th Conference on the Mechanical Behavior of Salt*. Institut National de l'Environnement Industriel et des Risques-ENERIS, France. pp.313–320.
- Luo, H., Laouafa, F., Guo, J. and Quintard, M. (2014). "Numerical modeling of three-phase dissolution of underground cavities using a diffuse interface model", *International Journal for Numerical and Analytical Methods in Geomechanics* (on-line), 38: 1600–1616. Doi:10.1002/nag.2274
- Meng, J., Chen, S., Wang, J., Chen, Z. and Zhang, J. (2023). "Experimental Study on the Dissolution Characteristics and Microstructure of Carbonate Rocks under the Action of Thermal–Hydraulic–Chemical Coupling", *Materials*, 16. Doi: 10.3390/ma16051828
- Min, N., Wang, M. L., Li, J., Guo, Y. and Gui, H. R. (2022). "Experimental study on water-rock interaction of limestone with different clay content constraints on the evolution of groundwater composition in limestone regions", *Fresenius Environmental Bulletin*, 31: 7703–7714.
- Molins, S., Soulaïne, C., Prasianakis, N. I., Abbasi, A., Poncet, P., Ladd, A. J. C., Starchenko, V., Roman, S., Trebotich, D., Tchelepi, H. A., & Steefel, C. I. (2021). "Simulation of mineral dissolution at the pore scale with evolving fluid-solid interfaces: review of approaches and benchmark problem set", *Computational Geosciences*, 25(4), 1285–1318. Doi:10.1007/s10596-019-09903-x
- Morse, J., & Mackenzie, F. (1990). *Geochemistry of sedimentary carbonates. Developments in sedimentology*, Amsterdam, New York: Elsevier.
- Novack, C. A., Anovitz, L. M., Hussey, D. S., LaManna, J. M. and Labotka, T. C. (2022). "Experimental Limestone Dissolution and Changes in Multiscale Structure Using Small- and Ultrasmall-Angle Neutron Scattering", *ACS Earth and Space Chemistry*, 6: 974–986. Doi: 10.1021/acsearthspacechem.1c00366
- Ogata, S., Yasuhara, H., Kinoshita, N., Cheon, D. S. and Kishida, K. (2018). "Modeling of coupled thermal-hydraulic-mechanical-chemical processes for predicting the evolution in permeability and reactive transport behavior within single rock fractures", *International Journal of Rock Mechanics and Mining Sciences* (on-line), 107: 271–281. Doi: 10.1016/j.ijrmms.2018.04.015
- Orgogozo, L., Golfier, F., Buès, M. and Quintard, M. (2010). "Upscaling of transport processes in porous media with biofilms in non-equilibrium conditions", *Advances in Water Resources*, 33: 585–600. Doi:10.1016/j.advwatres.2010.03.004
- Palmer A.N.1991 (2016). "Origin and morphology of limestone caves", *Geol Soc Am Bull* 103: 1-21. , 7606: 1–21. Doi: 10.1130/0016-7606(1991)103<0001:OAMOLC>2.3.CO;2

- Plummer, L. N., Wigley, T. M. L. and Parkhurst, D. L. (1978). "Kinetics of calcite dissolution in CO₂-Water systems at 5 degree TO 60 degree C and 0. 0 to 1. 0 atm CO₂", *Am J Sci*, 278: 179–216.
- Schabernack, J. and Fischer, C. (2022). "Improved kinetics for mineral dissolution reactions in pore-scale reactive transport modeling", *Geochimica et Cosmochimica Acta* (on-line), 334: 99–118. Doi:10.1016/j.gca.2022.08.003
- Sheng, Q. (2013). "*Pore-To-Continuum Multiscale Modeling of Two-Phase Flow in Porous Media*", PhD Thesis, University of Tianjin.
- Shovkun, I. and Espinoza, D. N. (2019). "Propagation of toughness-dominated fluid-driven fractures in reactive porous media", *International Journal of Rock Mechanics and Mining Sciences* (on-line), 118: 42–51. Doi: 10.1016/j.ijrmms.2019.03.017
- Taheri, K., Parvizi, F. and Valizadeh R. (2005). "Introduction to Hamedan sinkhols", published by Iranian Company of Gharb Regional Water in persian.
- Taheri, K., Gutiérrez, F., Mohseni, H., Raeisi, E. and Taheri, M. (2015). "Sinkhole susceptibility mapping using the analytical hierarchy process (AHP) and magnitude-frequency relationships: A case study in Hamadan province, Iran", *Geomorphology* (on-line), 234: 64–79. Doi: 10.1016/j.geomorph.2015.01.005
- Waltham, T., Bell, F., Culshaw, M. (2005). "*Sinkholes and subsidence*", Springer.
- Wang, Q., Zhang, F., Huang, R., Wang, X., Yang, C., Wang, H. and Qiu, T. (2020). "Multiphase flow and multicomponent reactive transport study in the catalyst layer of structured catalytic packings for the direct hydration of cyclohexene", *Chemical Engineering and Processing - Process Intensification*, 158. Doi: 10.1016/j.cep.2020.108199
- Wang, Y., Chai, J., Xu, Z., Qin, Y. and Wang, X. (2020). "Numerical simulation of the fluid-solid coupling mechanism of internal erosion in granular soil", *Water (Switzerland)*, 12. Doi: 10.3390/w12010137
- Xiao-Lei, L., Xin-Lei, L., Yue, W., Wei-Hang, P., Xuan, F., Zheng-Zheng, C. and Rui-Fu, L. (2023). "The Seepage Evolution Mechanism of Variable Mass of Broken Rock in Karst Collapse Column under the Influence of Mining Stress", *Geofluids*, 2023. Doi: 10.1155/2023/7256937
- Zhang, K. N., Zhu, K. F., He, Y. and Zhang, Y. Y. (2022). "Experimental study on karst development characteristics of calcrite and analysis of its dissolution mechanism", *Carbonate and Evaporites*, 37. Doi: 10.1007/s13146-022-00787-0
- Zhang, Q., Deng, H., Dong, Y., Molins, S., Li, X. and Steefel, C. (2022). "Investigation of Coupled Processes in Fractures and the Bordering Matrix via a Micro-Continuum Reactive Transport Model", *Water Resources Research*, 58: 1–18. Doi: 10.1029/2021WR030578
- Zhang, Z., Jiang, D., Liu, W., Chen, J., Li, E., Fan, J. and Xie, K. (2019). "Study on the mechanism of roof collapse and leakage of horizontal cavern in thinly bedded salt rocks", *Environmental Earth Sciences* (on-line), 78: 1–13. Doi: 10.1007/s12665-019-8292-2
- Zhao, C. bin, Hobbs, B. and Ord, A. (2018). "Effects of different numerical algorithms on simulation of chemical dissolution-front instability in fluid-saturated porous rocks", *Journal of Central South University*, 25: 1966–1975. Doi: 10.1007/s11771-018-3887-4

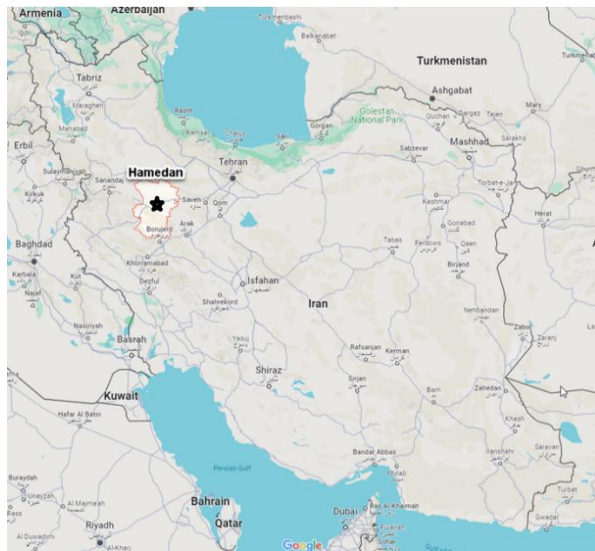


Figure 1. Location of Hamedan city in Iran map

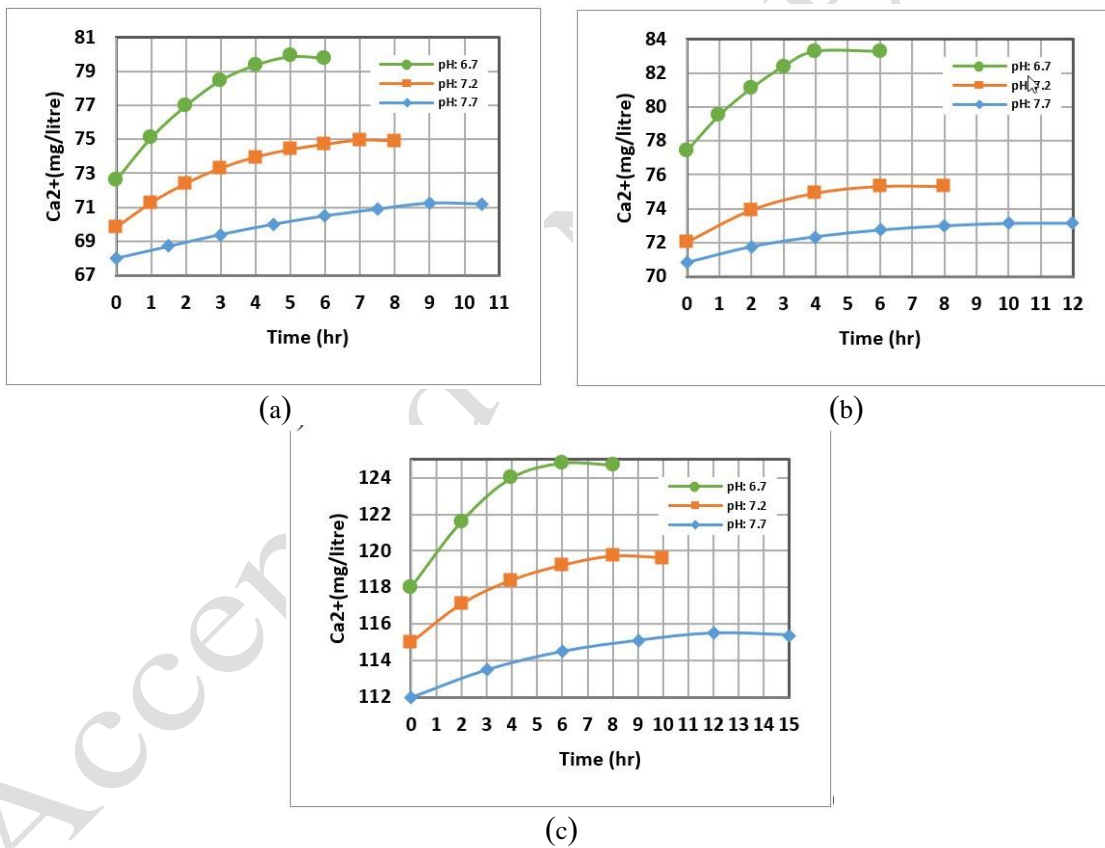


Figure 2. Changes in the concentration of calcium ions measured in the laboratory for the regions of a) Hamekasi b) Ali Sadr c) Abshineh (Dousti, 2009)

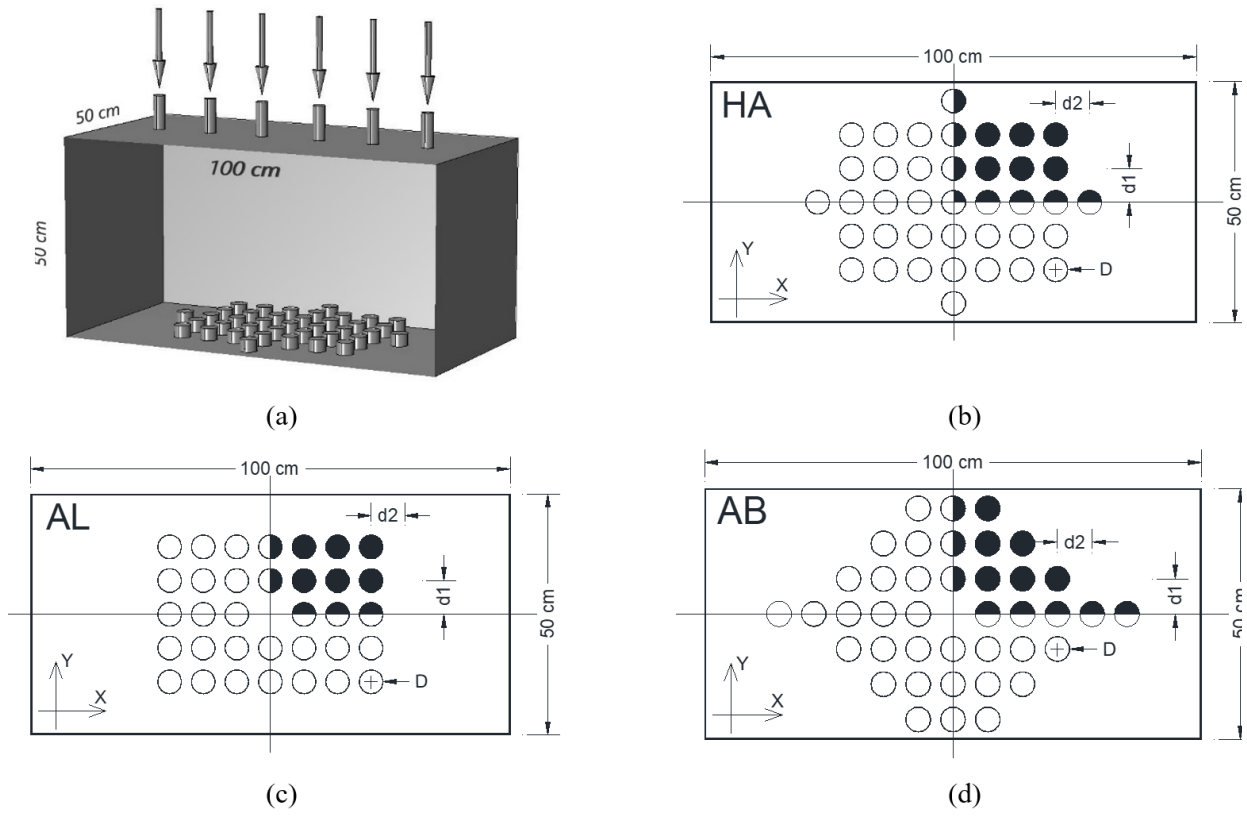


Figure 3. a) tank and samples situation, and samples arrangement in plane for the regions of b) Hamekasi c) Ali Sadr d) Abshineh

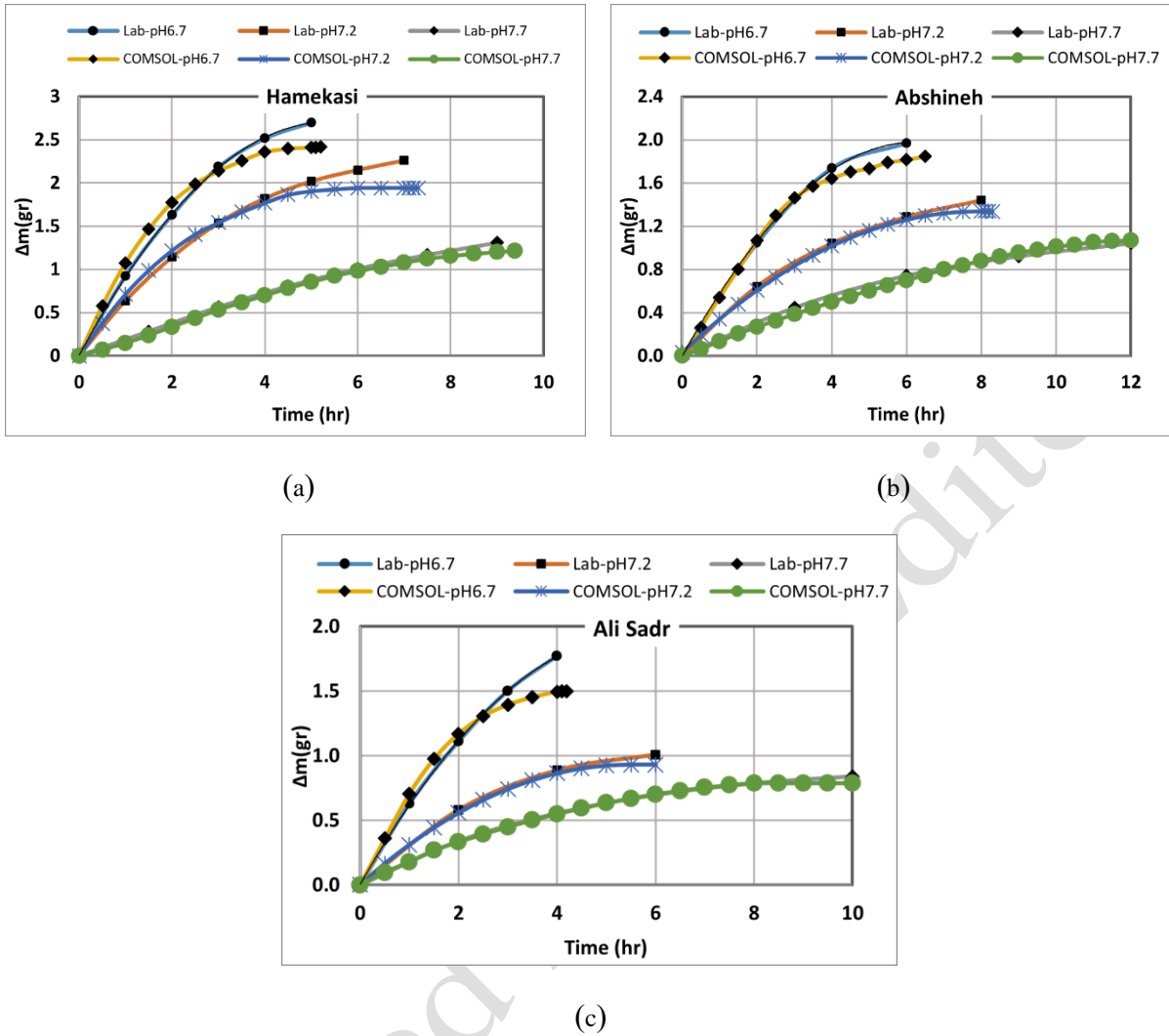


Figure 4. Laboratory results and numerical simulations of samples from the regions of a) Hamekasi b) Abshineh c) Ali Sadr

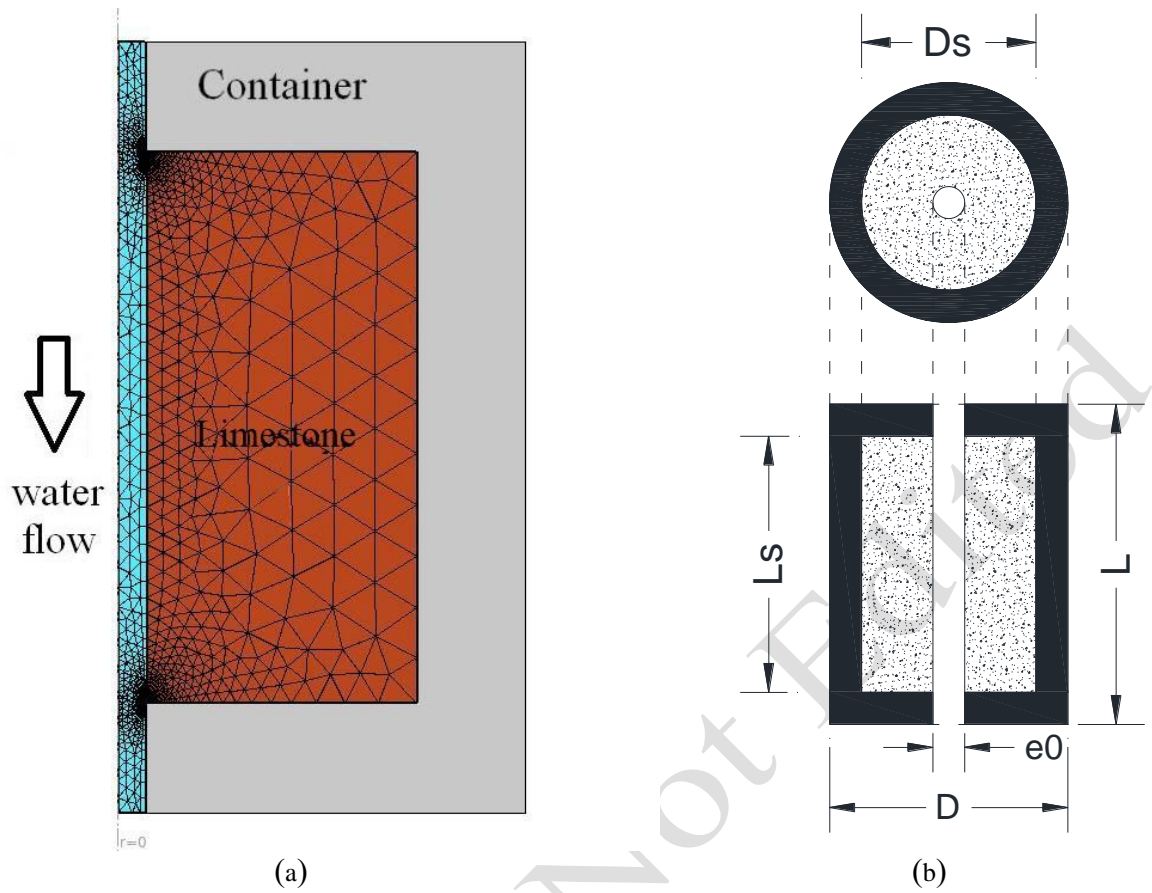


Figure 5. a) Sample meshing in COMSOL Multiphysics, b) Schematic model of the vertical hole and water flow in limestone

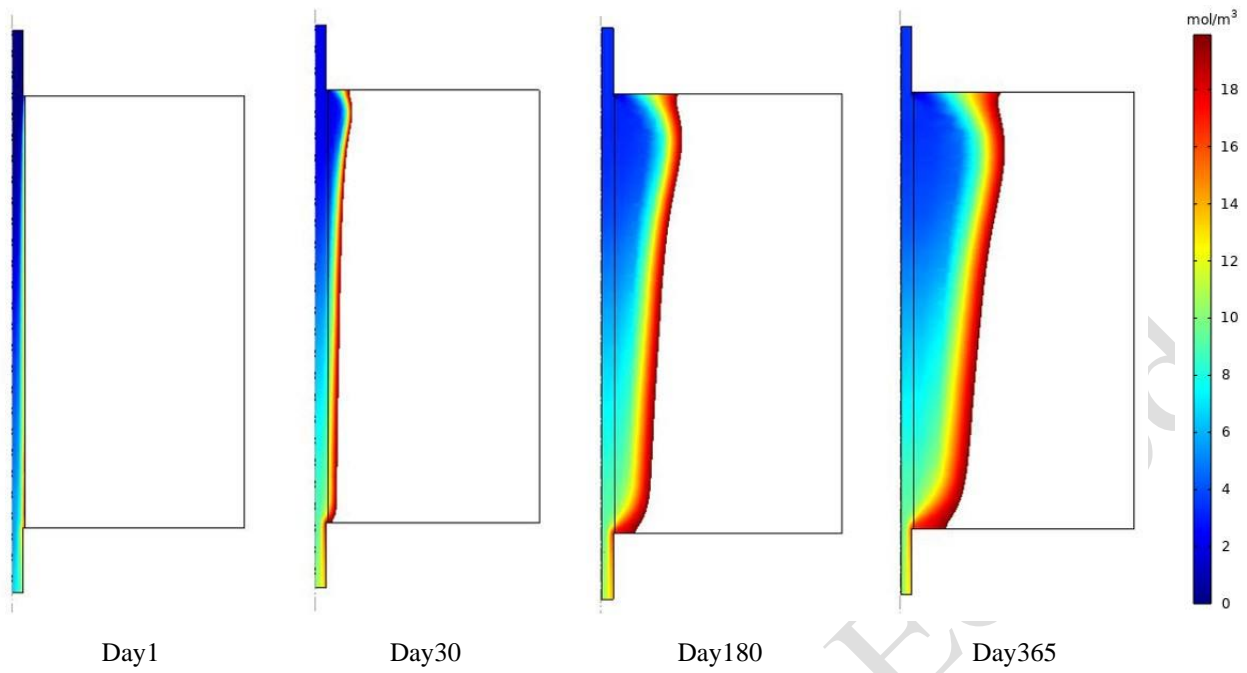


Figure 6. Evolution of hole diameter for Hamekasi region during time under conditions of $\text{pH}=6.7$, $e_0=3\text{mm}$ and $\text{Pe}=1e4$ (the colors show concentration of calcium ions in mol/m^3)

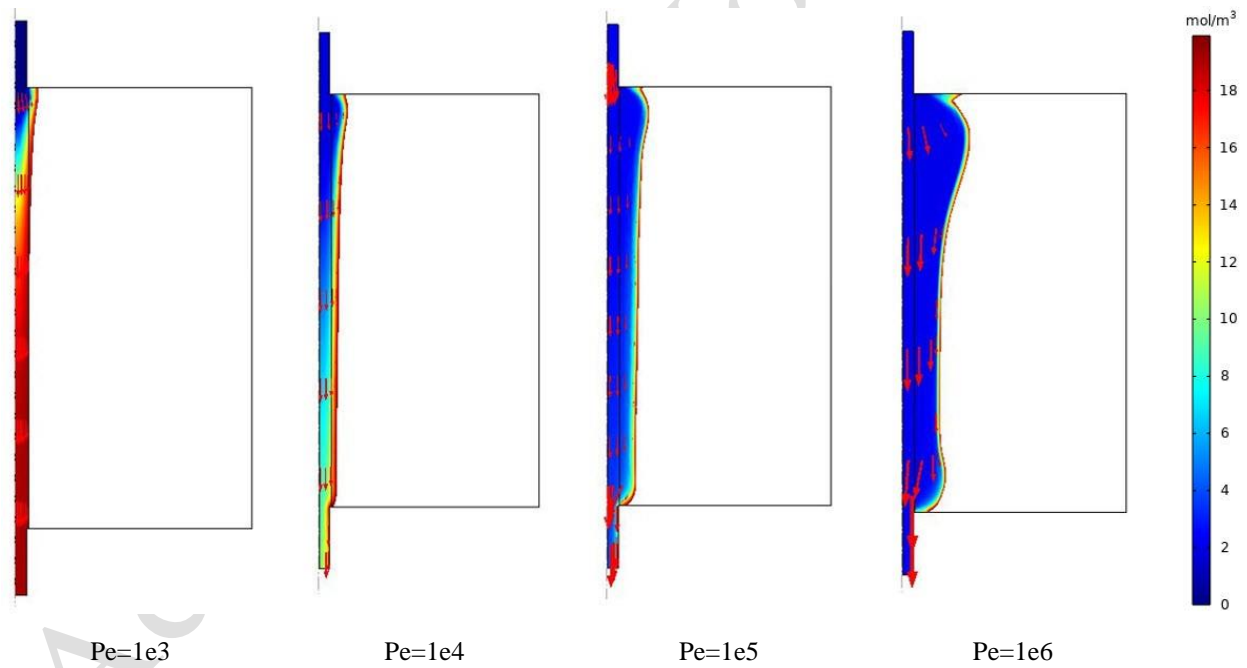
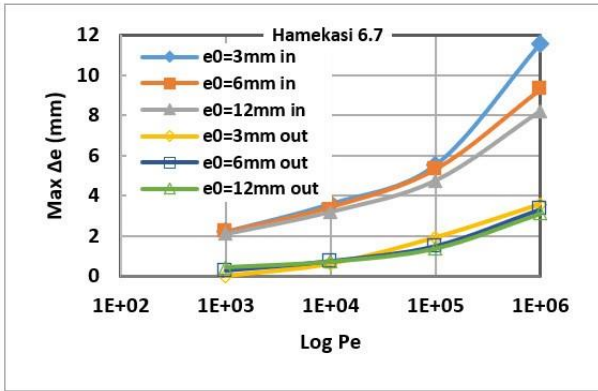
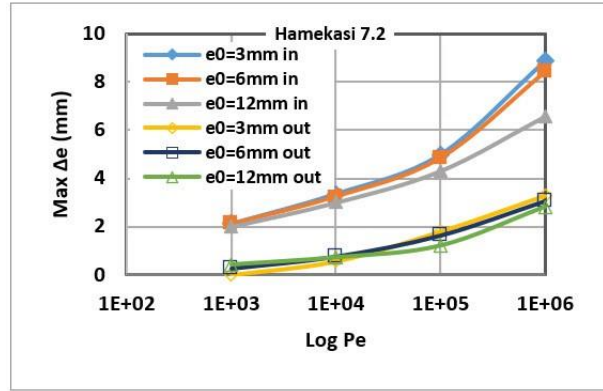


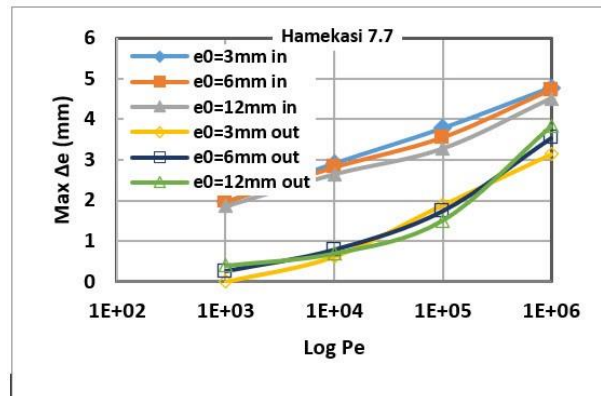
Figure 7. The change in the hole diameter in terms of Peclet number at the end of 16th day of dissolution for Hamekasi region under the conditions of initial diameter of 3mm and $\text{pH}=6.7$ (the colors show concentration of calcium ions in mol/m^3)



(a)



(b)



(c)

Figure 8. The changes in hole diameter at the end of 16th day of dissolution for Hamekasi region in terms of different acidic conditions of a) pH=6.7 b) pH=7.2 and c) pH=7.7

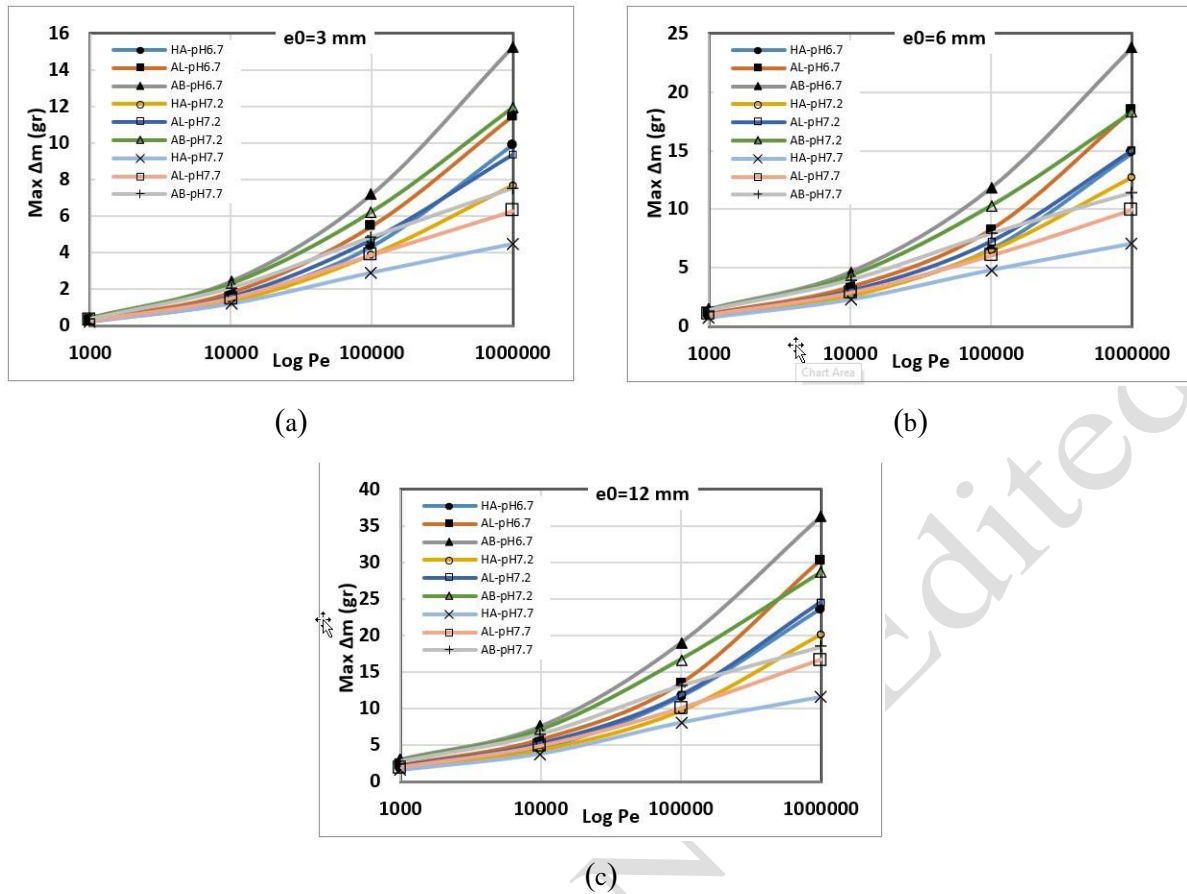


Figure 9. Dissolved mass of holes in terms of Peclet number at the end of 16th day for different acidic conditions and initial diameters of a) $e_0=3\text{mm}$ b) $e_0=6\text{mm}$ and c) $e_0=12\text{mm}$

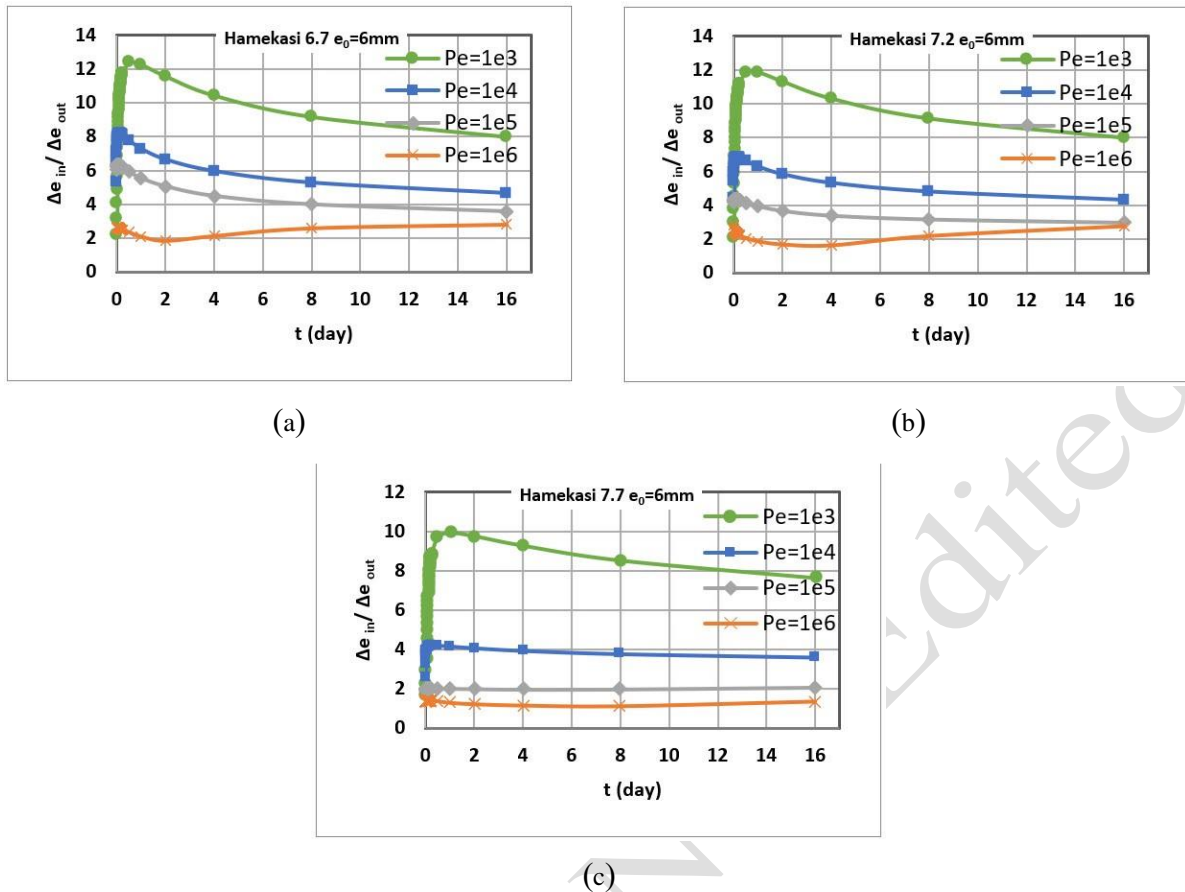


Figure 10. Changes in the inlet to outlet widths ratio of Hamekasi region for the hole initial diameter of 6mm and different acidic conditions of a) pH=6.7 b) pH=7.2 c) pH=7.7

Table 1. Summarized experimental data on samples of the three studied regions

Study area	pH	Initial concentration of calcium ions in water (mg/liter)	Calcium ion concentration in saturated state (mg/liter)	Time required for saturation (hr)	Laboratory dissolution rate constant (10^{-5} m/s)	The total mass reduction of all samples (gr)
Hamekasi	6.2	72.60	79.90	5	6.15	2.70
	7.2	69.80	74.95	7	5.11	2.26
	7.7	68.00	71.25	9	3.23	1.31
Ali Sadr	6.2	77.40	83.30	4	6.34	1.77
	7.2	72.00	75.30	6	4.33	1.01
	7.7	70.80	73.15	10	3.03	0.84
Abshineh	6.2	118.00	124.70	6	3.87	1.97
	7.2	115.00	119.70	8	2.98	1.44
	7.7	112.00	115.50	12	1.93	1.04

Table 2. Dissolution parameters obtained from the calibration on experimental results

Study area	pH	Dissolution rate constant k_s ($10^{-2}mol/(m^2 \cdot s)$)	Reaction order n
Hamekasi	6.2	2.316	0.50
	7.2	1.446	0.50
	7.7	0.590	0.47
Ali Sadr	6.2	2.222	0.48
	7.2	1.470	0.50
	7.7	0.731	0.50
Abshineh	6.2	2.347	0.50
	7.2	1.411	0.50
	7.7	0.782	0.50

Accepted / Not Edited